REDUCING THE COMPLEXITY OF ORTHOGONAL CODE BASED SYNTHETIC APERTURE ULTRASOUND SYSTEMS*

Ming Yang, Siyuan Wei and Chaitali Chakrabarti

School of Electrical, Computer and Energy Engineering
Arizona State University, Tempe, AZ 85287
email: {m.yang, siyuan.wei, chaitali}@asu.edu

ABSTRACT

In this paper, we propose several techniques to reduce the computation complexity of orthogonal chirp and orthogonal Golay code based synthetic aperture ultrasound systems. First, we minimize the complexity in terms of number of effective multiplications by choosing the system parameters for a specified SNR gain. The proposed method helps in reducing the complexity by about $20\times$. Next, we consider a system that compensates for body motion. We reduce the complexity of motion compensation first by doing the calculations in polar domain, and second, by making use of the correlation in motion velocity field in a small neighborhood. These approximations reduce the computation complexity by $3000\times$ with minimal performance penalty.

Index Terms— Synthetic aperture ultrasound, orthogonal coded excitation, Golay code, chirp, motion compensation

1. INTRODUCTION

Synthetic Aperture Ultrasound (SAU) is a popular technique for ultrasound imaging. Compared to conventional phased array ultrasound systems, SAU can produce high resolution images with very high frame rates because the frame rate of an SAU system does not depend on number of scanlines [1].

However, classic SAU systems suffer from significant SNR loss due to the fact that only one transmit element is fired during each transmission. Orthogonal coded excitation such as orthogonal Golay code [2] and orthogonal chirp [3] allow for multiple transmissions and are suitable for such systems. Both Golay code and chirp based systems have significant improvement in SNR and penetration depth. However, such systems are also sensitive to body motion, because the performance of these systems rely on perfect timing alignment.

In our earlier work [4], we proposed a reduced complexity beamforming architecture for orthogonal Golay and chirp based SAU systems. The architecture was capable of dynamically adjusting beamforming delay according to motion velocity, so that motion artifacts were significantly reduced. Unfortunately the motion compensation procedure in [4] required a large number multiplications and additions.

* This work was funded in part by grant NSF-CSR0910699.

In this paper we discuss several techniques to reduce the complexity of orthogonal code based SAU systems. Since the complexity of such a system is a function of N, the number receive elements, M, the number of transmit elements and L the code length, we first describe a framework to choose the value of these parameters such that the overall complexity is minimized for a given SNR gain. We consider both the number of multiplications and the number of additions in the formulation. We show that this procedure reduces the complexity of the system by about $20\times$. Next we reduce the complexity of the motion compensation method by first operating in the polar domain and then exploiting the property of uniformity of velocity field in a small region. This method helps reduce the complexity of motion compensation by $3000\times$. Finally we show that as a result of these reductions, the beamsum is now the bottleneck of orthogonal coded excitation based SAU systems.

The rest of the paper is organized as follows. Section 2 briefly reviews the beamforming architecture proposed in [4]. Section 3 describes the framework for choosing the parameters for the two orthogonal coded excitation systems. Section 4 proposes a low complexity motion compensation method that has very good performance. Section 5 concludes the paper.

2. SYSTEM OVERVIEW

The processing chains of a single receive channel of the beamforming architecture proposed for chirp-based and Golay code-based systems in [4] are shown in Fig. 1a and 1b respectively. The digitized signal is apodized and then interpolated by $3\times$ to increase the data sampling rate to 120MHz. The Golay based-system has two Golay correlators which generate two versions of correlated streams for decoding. The output of the interpolation filter in case of chirp-based system or the outputs of the two correlators in case of Golay code-based system, is stored in the front-end buffer for future processing by the beamforming unit.

The beamforming architecture is shown in Fig. 1c. This architecture integrates Hadamard decoding with beamforming and combines different signals corresponding to different transmit elements, different receive elements and different round trip delays. In presence of motion, the delay can be

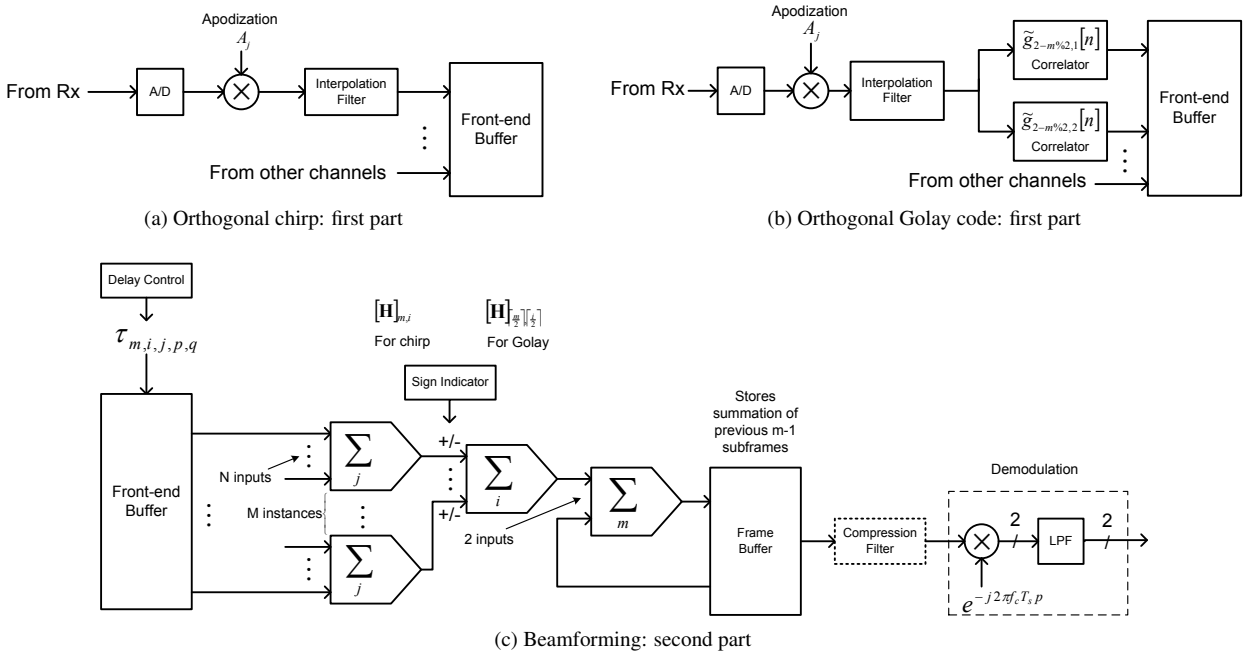

(a) Orthogonal chirp: first part

(b) Orthogonal Golay code: first part

(c) Beamforming: second part

Fig. 1: Front-end architectures for orthogonal chirp and Golay code based SAU systems

dynamically adjusted according to the motion velocity. There are three stages of summation. The first stage which consists of M summers, sum signal values from N receive elements. In the second stage, the signal samples corresponding to M transmit elements are summed up. The Hadamard matrices are used to decide whether to add or subtract the streams corresponding to the different transmission. This process is repeated for each transmission. In the third stage, the frame buffer updates the stored image frame with the image generated by the last transmission. The data in the frame buffer is demodulated. In case of a chirp-based system, there is a compression filter before the demodulation unit. Both compression filtering and demodulation are done scanline by scanline.

Table 1 gives the default parameter values of the proposed system. According to these values, the number of multiplications and additions per frame are calculated and shown in Table 2. It shows that in absence of motion, chirp compression filter contributes to 90% of the number of multiplications of a chirp-based system. In presence of motion, motion compensation dominates the complexity of both Golay code-based and chirp-based systems. In terms of number of additions, both beamsum and motion compensation contribute significantly to the complexity of Golay code based and chirp based systems.

3. PARAMETER SELECTION FOR COMPLEXITY REDUCTION

In this section we describe how the parameters N, M, L can be chosen to satisfy the performance requirements while minimizing the complexity. We define the reference system as one with only one transmit and one receive element, and

Table 1: Parameter definitions and values

Symbol	Description	Value
N	Number of receiving elements	128
M	Number of transmitting elements and number of transmissions	32
L	Code length, in times of the shortest sinusoid length	128
B	6dB bandwidth of transducer	4 MHz
f_s	A/D sampling frequency	40 MHz
f_s'	Sampling frequency after interpolation	120 MHz
K_{INT}	Number of taps of interpolation lowpass filter	5
D	Maximum detection depth	20 cm
c	Speed of sound in body tissue	1540 m/s
P	Number of focal points in one scanline	1.04×10^4
Q	Number of scanline in one image	200

with excitation of unit time-bandwidth product (TBP). We specify the performance requirement in terms of SNR gain which is defined as the ratio of the SNR of a system and the SNR of the reference system. It has been proven that longer code length of wide band signal results in higher TBP, and higher TBP contributes to higher SNR gain [5]. The number of transmissions and the number of simultaneous transmit elements also contributes to SNR gain [6]. Thus the theoretical SNR gain is approximately $10\log_{10}(NM^2L)$ dB for both chirp-based and Golay-based systems [3].

Since $M \leqslant N$, N determines the aperture size, and consequently the lateral resolution. Thus N should be chosen

Table 2: Complexity of each component per frame

Block name		Golay	Chirp
Interpolation filter	Mul	2.1×10^8	2.1×10^8
	Add	2.1×10^8	2.1×10^8
Golay correlation	Add	1.1×10^{10}	N/A
Compression filter	Mul	N/A	2.7×10^9
	Add	N/A	2.7×10^9
Beamsum	Add	2.72×10^{11}	2.72×10^{11}
Demodulation	Mul	7.9×10^7	7.9×10^7
	Add	1.5×10^8	1.5×10^8
Motion compensation	Mul	5.45×10^{11}	5.45×10^{11}
	Add	2.72×10^{11}	2.72×10^{11}

according to the desired lateral resolution. Axial resolution is hard to quantify. It is a function of system bandwidth, type of coded excitation and motion speed, and is not considered in the formulation below. Now for a given SNR gain constraint, there are multiple choices of M and L. In the following, we formulate this as an optimization problem which minimizes computation complexity given SNR gain constraint $NM^2L \geqslant A$, where $L \in [L_{min}, L_{max}]$ and $M \in [M_{min}, M_{max}]$. In our system, $L_{min} = 1$, $L_{max} = 128$, $M_{min} = 1$ and $M_{max} = 64$.

Optimization of Golay code-based system:

For the Golay code based system, the computation complexity is given by

$$K_{INT}PNM+\alpha[K_{INT}PNM+PQNM^2+2PNML] \quad (1)$$

Here $K_{INT}PNM$ is the number of multiplications and additions required by the interpolation filter, $PQNM^2$ is the number of additions needed by the beamsum unit, and $2PNML$ is the number of additions for the Golay correlation units. We combine the effect of multiplications and additions by scaling the number of additions by a constant α, where α is the ratio of the complexity of an adder to the complexity of a multiplier. For a 16-bit-fixed-point system, that range of α varies from 1/14 to 1/8, depending on the specifics of the adder and multiplier implementations. In this paper, we use $\alpha = 1/12$ to evaluate the complexity.

Optimization of chirp-based system:

For the chirp-based system, the complexity is given by

$$\begin{aligned} &K_{INT}PNM + PQL_0L + \alpha[K_{INT}PNM \\ &+ PQNM^2 + PQL_0L] \end{aligned} \quad (2)$$

where $K_{INT}PNM$ is the number of multiplications and additions in the interpolation filter, $PQNM^2$ is the number of additions in the beamsum unit and PQL_0L the number of multiplications and additions in the compression filter with L_0L taps. Here L_0 is the number of samples in one period of a sinusoid whose frequency is the same as the transducer's central frequency.

FFT-based compression filtering:

Since complexity of the chirp compression filter is very high and the number of taps can be as high as 1280, we propose to use FFT for filter implementation. We use the overlap-save method, where the signal is divided into s chunks of equal length, and length of FFT U is chosen according to $U = 2^{\lceil \log_2(L_0L+(L_0L+P)/s-1)\rceil}$. For this implementation the number of multiplications per scanline is $s(2U \log_2 U + 2U)$, and the number of additions per scanline is $s(3U \log_2 U + U)$. The computation complexity of chirp based system using FFT-based compression filter is given by

$$\begin{aligned} &K_{INT}PNM + Qs(2U \log_2 U + 2U)+ \\ &\alpha[K_{INT}PNM + PQNM^2 + Qs(3U \log_2 U + U)] \end{aligned} \quad (3)$$

Complexity Results:

Fig. 2 plots the number of effective multiplications for different values of SNR gain for the two systems. We see that the complexity of the system is proportional to the SNR gain as expected. The step shape is caused by the constraint that M is an integer power of 2 — a constraint that is set by the Hadamard matrix required to generate orthogonal codes. We repeated this experiment for $\alpha = 1/8$ and $\alpha = 1/16$. We find that the optimal values of M, L do not change with α. This is because the constraint that M has to be an integer power of 2 is a strong constraint and changing the value of α has little effect on the choice of the parameters M and L.

To evaluate the optimization efficiency, we compare the complexity of the optimal solution with the average of all feasible solutions for a specific SNR gain. Fig. 3a and 3b show the comparison result of the average versus the optimal configuration for five different SNR constraints. The complexity of the optimal solution is only 5.8% of the average for Golay code based system and 5.5% of the average for chirp based system. Of all the units, the beamsum is the most complex with a complexity of 99% for chirp based system and 98% for Golay code based systems. The reduction in the number of computations for beamsum is quite significant. For 60dB SNR gain, the number of effective multiplications for optimized beamsum is only 4.7% of those needed by the average. The complexity reduction of each unit is summarized in Table 3.

Simulation Results:

All the simulations in this paper are based on the Field II ultrasound simulation tool [7, 8]. Fig.4 shows the simulation results for five values of SNR gain. Here we consider one single point target 10cm under the transducer array.

We see that in presence of motion, Golay code based system suffers the most. Chirp-based system also has significant SNR loss when SNR gain constraint is higher than 70dB. This is because orthogonal code based SAU systems require perfect timing alignment to insure the signal coherency and

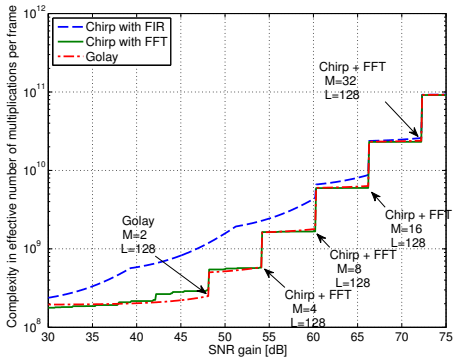

Fig. 2: Choice of M and L to achieve lowest complexity for different values of SNR gain

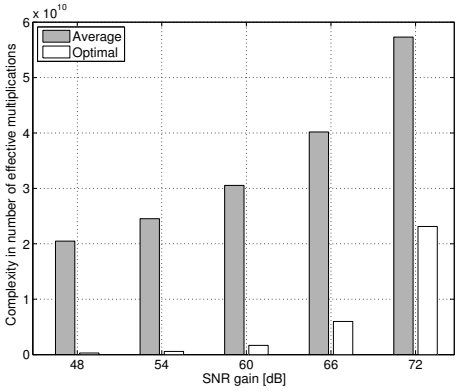

(a) Chirp-based system

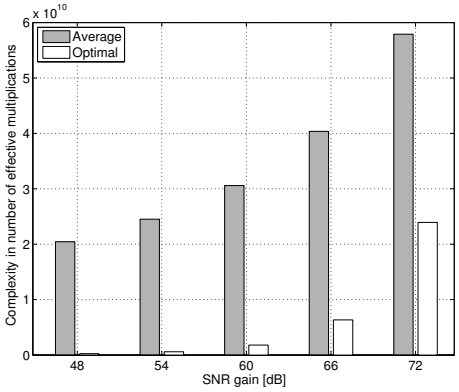

(b) Golay code-based system

Fig. 3: Complexity comparison between average and optimal configuration ofcChirp and Golay code based system

sidelobe suppression. Thus to design a high performance system, motion compensation has to be included.

4. SIMPLIFIED MOTION COMPENSATION METHOD

Body motion results in alignment errors in SAU beamforming. This can be compensated by dynamically adjusting the delay according to motion velocity, as described in [9]. In

Table 3: Complexity reduction for 60dB SNR gain case

Component	Golay Avg.	Golay Opt.	Percentage
Interpolation	2.1×10^8	5.8×10^7	27.6%
Beamsum	3.0×10^{10}	1.4×10^9	4.7%
Correlation	1.1×10^8	2.3×10^8	209%
Demodulation	9.2×10^7	9.2×10^7	100%
Total	3.1×10^{10}	1.8×10^9	5.8%
Component	**Chirp Avg.**	**Chirp Opt.**	**Percentage**
Interpolation	2.1×10^8	5.8×10^7	27.6%
Beamsum	3.0×10^{10}	1.4×10^9	4.7%
Correlation	6.9×10^7	1.0×10^8	145%
Demodulation	9.2×10^7	9.2×10^7	100%
Total	3.1×10^{10}	1.7×10^9	5.5%

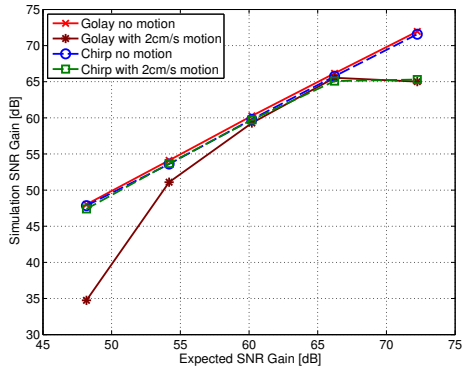

Fig. 4: SNR gain in presence of motion

our previous work [4], we used Taylor expansion to simplify the calculation in motion compensation. Unfortunately, the complexity of that method is still very high. In this section, we propose a scheme that reduces the complexity by first doing the computations on data represented in the polar system and second by assuming uniformity of velocity field in a small region.

4.1. Mapping Computations into Polar Domain

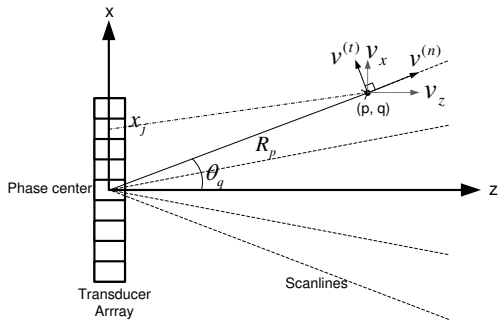

Fig. 5: Motion decomposition using polar coordinates

We propose to represent the motion velocity in polar

coordinates instead of rectangular coordinates with v_x and v_y as shown in Fig. 5. Such a representation is better in terms of both computation and storage complexity.

Suppose the target at point (p, q) is moving, so the distance $R_{p,q}$ and the angle $\theta_{p,q}$ vary with time. The two new velocity components are defined as $v_{p,q}^{(n)} = \frac{dR_{p,q}}{dt}$ and $v_{p,q}^{(t)} = R_{p,q}\frac{d\theta_{p,q}}{dt}$, where $v_{p,q}^{(n)}$ is parallel to the scanline and $v_{p,q}^{(t)}$ is vertical to the scanline.

We find that when $R_{p,q}$ is large, the derivative of single trip delay from point (p, q) to receive element j can be approximated by equation (4), where x_j is the coordinate of the receive element j.

$$\frac{d\tau_{rx}}{dt} \approx \frac{1}{c}v_{p,q}^{(n)} - \frac{x_j \cos\theta_{p,q}}{cR_{p,q}}v_{p,q}^{(t)} \quad (4)$$

For the round trip delay from transmit element i to point (p, q) to receive element j, the approximation of the total delay adjustment term for mth transmission is represented by

$$\Delta\tau_{m,i,j,p,q} \approx \frac{2}{c}v_{p,q}^{(n)}m\Delta t - \frac{(x_j + x_i)\cos\theta_{p,q}}{cR_{p,q}}v_{p,q}^{(t)}m\Delta t \quad (5)$$

where x_i is the x coordinate of the ith transmit element, Δt is the transmit interval between two consecutive transmissions, m is the index of transmission which varies from 0 to $M-1$

To ensure good accuracy at small depths, only a few transmit/receive elements near the center are used. Since here the signal strength is good, this operation incurs only a mild performance loss. As the distance $R_{p,q}$ increases, more streams are used for beamforming. Simulation results show that $\frac{R_{p,q}}{\max(|x_i|,|x_j|)} > 3$ reaches a balance between approximation accuracy and performance loss due to reduction in the aperture size.

4.2. Neighborhood Approximation

Body motion is likely to have significant regional correlation. In abdominal ultrasound imaging, the most likely motion is caused by patient's breathing or moving of transducer head. As a result, it is reasonable to assume that the velocity field generated by body motion is continuous and locally correlated. Based on this assumption, delay adjustment term due to motion does not have to be calculated for every focal point, and can be calculated once in every local neighborhood.

In this paper, we use a simple deformation velocity field to simulate a mild body motion [10]. The velocity field shown in Fig. 6a corresponds to the case where the tissues are being compressed in the vertical direction and being expanded in the horizontal direction. In motion fields where the velocity vectors have similar orientations, the neighborhood approximation has very good performance even for grid sizes as large as 200×5 (200 samples along the scanline and 5 scanlines wide). However in the motion field investigated in this paper, the motion vectors are in all possible directions in the 2D plane. In this case, even some small neighborhood

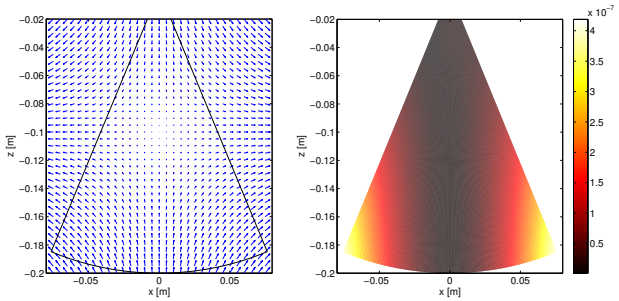

(a) Simulation velocity field (b) Neighborhood approximation error

Fig. 6: Velocity field and neighborhood approximation error when the neighborhood is of size 20×3

size such as 50×1 or 30×5 results in large Range Sidelobe Level (RSLL). In the worst case where motion speed reaches 20mm/s, the RSLL is larger than -41dB. As a result, smaller grid size is necessary for such a motion field. To choose a good grid size, we further tested grid sizes of 10×6, 20×3 and 30×2. All three configurations provide acceptable performance and have the same reduction in complexity. However, when motion speed is 20mm/s, 20×3 neighborhood approximation has about 3dB better performance than the other two cases and approaches the performance of motion compensation without approximation. The mean square error of the delay values in each neighborhood is shown in Fig. 6b. In this configuration the highest mean square error is proportional to 4.2×10^{-7}, and occurs in the bottom two corners.

4.3. Complexity Analysis

We first analyze the number of multiplications and additions that are required to compute Equation (5). The first term in the equation does not depends on i or j, which means it can be shared by all streams. As a result, this part only needs 1 multiplications per focal point, so if we recalculate the delay for every subframe, PQM multiplications are required for one image. The second term is a linear function of $x_i + x_j$. When elements are equally spaced, one can calculate the second term with only add/subtract according to the adjustment term used in $i-1$ or $j-1$ streams. As a result, this part needs PQM multiplications and PQM^2N addition per frame. Compared to the motion compensation in [4], the number of multiplications needed is only 0.12% of that method.

Now, for the neighborhood approximation method, there are $P'Q' = PQ/(20 \times 3)$ small neighborhoods, and the samples in the same neighborhood can share the same adjustment term. Taking this into account, the new motion compensation needs $2P'Q'M$ multiplications and $2P'Q'M^2N$ additions per frame. Compared to the method in [4] using the same configuration, the total number of effective multiplications needed by motion compensation is reduced from 6.8×10^{11} per frame to 2.3×10^8 per frame, which corresponds to about

$3000\times$ reduction.

4.4. Simulation results

We ran simulations for the gradient field described in Fig. 6a for maximum motion speed varying from 0 mm/s to 20 mm/s. We put 30 target points in the observation area; the space between each point is 30mm along range direction and 10° along the azimuth direction.

Fig. 7 and 8 show the average SNR performance and average RSLL performance of 30 target points for different motion speeds. As shown in Fig.7, the new reduced complexity motion compensation method can significantly improve the SNR for both Golay code and chirp based systems. The SNR performance of Golay code based systems is slightly better than a chirp based system.

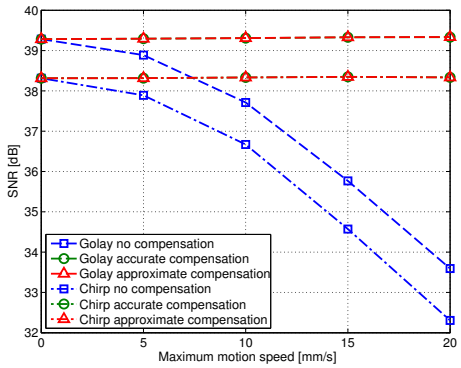

Fig. 7: SNR performance for different motion speed

From Fig. 8 we see that for both Golay code based and chirp based systems, the RSLL performance of the simplified motion compensation method is very close to the one without the approximations.

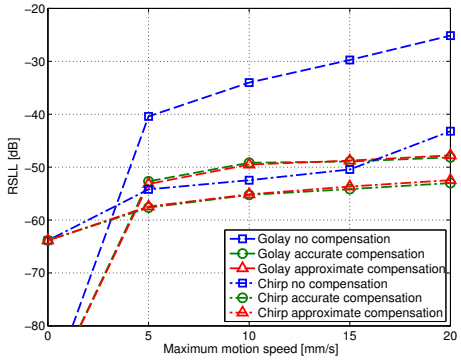

Fig. 8: RSLL performance for different motion speed

5. CONCLUSION

This paper focuses on reducing the complexity of orthogonal Golay and chirp based SAU systems. First, we determine the values of M and L so that the number of effective multiplications for a given SNR gain constraint is minimized. We use the FFT based method to reduce the complexity of chirp compression filter. The proposed method helps in reducing the complexity by 94-95%. Next we propose a new way to calculate the motion compensation adjustment term by doing all computations on polar data and by exploiting the fact that the velocity field is constant in a small neighborhood. By using the new method, the complexity of the motion compensation part is reduced by about $3000\times$. As a result of the proposed reductions, the overall complexity of the orthogonal code based SAU system is dominated by beamsum and not by motion compensation.

6. REFERENCES

[1] C.R. Hazard and G.R. Lockwood, "Theoretical assessment of a synthetic aperture beamformer for real-time 3-d imaging," *IEEE Transactions on Ultrasonics, Ferroelectrics and Frequency Control*, vol. 46, no. 4, pp. 972–980, 1999.

[2] R.Y. Chiao and L.J. Thomas, "Synthetic transmit aperture imaging using orthogonal Golay coded excitation," in *Proceedings of IEEE Ultrasonics Symposium*, Oct. 2000, vol. 2, pp. 1677 –1680.

[3] T. Misaridis and J.A. Jensen, "Use of modulated excitation signals in medical ultrasound. part III: high frame rate imaging," *IEEE Transactions on Ultrasonics Ferroelectrics and Frequency Control*, vol. 52, no. 2, pp. 208 –219, Feb. 2005.

[4] M. Yang and C. Chakrabarti, "Design of orthogonal coded excitation for synthetic aperture imaging in ultrasound systems," in *IEEE International Symposium on Circuits and Systems*, May 2012.

[5] T. Misaridis and J.A. Jensen, "Use of modulated excitation signals in medical ultrasound. part I: basic concepts and expected benefits," *IEEE Transactions on Ultrasonics, Ferroelectrics and Frequency Control*, vol. 52, no. 2, pp. 177 –191, Feb. 2005.

[6] R.Y. Chiao, L. J. Thomas, and S.D. Silverstein, "Sparse array imaging with spatially-encoded transmits," in *Proceedings of IEEE Ultrasonics Symposium*, Oct. 1997, vol. 2, pp. 1679–1682.

[7] J. A. Jensen, "Field: A program for simulating ultrasound systems," in *10th Nordicbaltic Conference on Biomedical Imaging, Vol. 4, Supplement 1, Part 1:351–353*, 1996, pp. 351–353.

[8] J.A. Jensen and N.B. Svendsen, "Calculation of pressure fields from arbitrarily shaped, apodized, and excited ultrasound transducers," *IEEE Transactions on Ultrasonics Ferroelectrics and Frequency Control*, vol. 39, no. 2, pp. 262 –267, Mar 1992.

[9] S. Nikolov, K. Gammelmark, and J. Jensen, "Velocity estimation using recursive ultrasound imaging and spatially encoded signals," in *IEEE Ultrasonics Symposium*, 2000, vol. 2, pp. 1473 –1477.

[10] J. Meunier and M. Bertrand, "Ultrasonic texture motion analysis: theory and simulation," *IEEE Transactions on Medical Imaging*, vol. 14, no. 2, pp. 293 –300, June 1995.